ACS APPLIED MATERIALS & INTERFACES

Research Article

www.acsami.org

Artificial Chaperones Based on Mixed Shell Polymeric Micelles: Insight into the Mechanism of the Interaction of the Chaperone with Substrate Proteins Using Förster Resonance Energy Transfer

Jianzu Wang, Tao Yin, Fan Huang, Yiqing Song, Yingli An, Zhenkun Zhang,* and Linqi Shi*

State Key Laboratory of Medicinal Chemical Biology, Key Laboratory of Functional Polymer Materials, Ministry of Education, Institute of Polymer Chemistry, Collaborative Innovation Center of Chemical Science and Engineering (Tianjin), Nankai University, Tianjin 300071, China

Supporting Information

ABSTRACT: Controlled and reversible interactions between polymeric nanoparticles and proteins have gained more and more attention with the hope to address many biological issues such as prevention of protein denaturation, interference of the fibrillation of disease relative proteins, removing of toxic biomolecules as well as targeting delivery of proteins, etc. In such cases, proper analytic techniques are needed to reveal the underlying mechanism of the particle-protein interactions. In the current work, Förster Resonance Energy Transfer (FRET) was used to investigate the interaction of our tailor designed artificial chaperone based on mixed shell polymeric micelles (MSPMs) with their substrate proteins. We designed a new kind of MSPMs with fluorescent acceptors precisely placed at the desired locations as well as hydrophobic domains which can adsorb unfolded proteins with a propensity to aggregate. Interactions of such model micelles with a donor-labeled protein-FITC-lysozyme, was monitored by FRET. The fabrication strategy of MSPMs makes it possible to control the accurate location of the acceptor, which is critical to reveal some unexpected insights of the micelle-protein interactions upon heating and cooling. Preadsorption of native proteins onto the hydrophobic domains of the MSPMs is a key step to prevent thermo-denaturation by diminishing interprotein aggregations. Reversible protein adsorption during heating and releasing during cooling have been confirmed. Conclusions from the FRET effect are in line with the measurement of residual enzymatic activity.

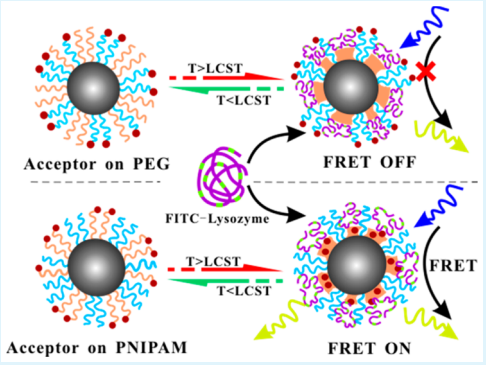

KEYWORDS: *artificial chaperone, mixed shell polymeric micelle, Förster resonance energy transfer, protein, nanoparticle*

1. INTRODUCTION

With their huge potentials in targeting drug delivery, bioimaging and diagnosis, polymer based nanoparticles (NPs), together with NPs of other materials, have been boosting the development of nanomedicine.[1,2] It is generally accepted that nanoparticles are immediately covered with a protein corona right after being exposed to a biological fluid.[3] The protein corona can influence blood circulation, transportation, and targeting properties of NPs, usually resulting in under-expected performance. Therefore, on the one hand, to avoid nonspecific protein-nanoparticle interactions is a key issue that has been tackled from different perspectives.[4−6] On the other hand, there are also immerging trends in recent years to wisely exploit protein−nanoparticle interactions with the hope to extend the application of polymer based nanoparticles into many other important biological issues,[3,4] such as prevention of protein denaturation,[7,8] interference of the fibrillation of Alzheimer-disease relative amyloid beta-proteins,[9] removing of toxic biomolecules,[10] delivery of protein-based biomedicines,[11−13] and enrichment of valuable low-abundance proteins,[14] just name a few. The key in such applications is to introduce controlled and reversible interactions between the nanoparticles and proteins of interest, of which many progresses have been made in the past decades.[3,15,16] For instance, Shea and co-workers have synthesized a library of polymer-based NPs which can interact with biomolecules such as peptides, proteins and heparins with high selectivity.[7,10,17,18] Controlled interactions between proteins and NPs based on responsive block polymers have been exploited by Liu's group for a wide range of applications.[13] Novel cholesteryl group-bearing pullulan based cationic nanogels developed by Akiyoshi and co-workers can complex with a number of proteins which can further be released by adding cyclodextrin strippers.[19] Core−shell colloidal particles with a thermo and pH responsive shell exhibited controlled interactions with model proteins.[20] We have also developed polymeric micelles with a tunable surface, which have been used to prevent a wide spectrum of proteins with varied structure complexity from heating-

Received: January 22, 2015
Accepted: May 4, 2015
Published: May 4, 2015

DOI: 10.1021/acsami.5b00684
ACS Appl. Mater. Interfaces 2015, 7, 10238−10249

denaturation.[8] Recently, we succeeded in applying such system to delay the harmful fibrillation of amyloid-beta proteins, a key peptide in Alzheimer's disease.[21]

The general characteristic of the aforementioned systems is that the nanoparticle−protein interacting process is highly dynamic: the polymeric particles are in the dormant state and no interaction between the particles and proteins exist until some external stimuli are applied. Furthermore, the bound proteins can be purposely released from the nanoparticle surface. To achieve better control of such dynamic process, the current challenge is to monitor such stimulus responsive interactions and to reveal the underlying mechanism of interactions.[22,23] So far many techniques have been recruited for such goals,[16,24,25] including circular dichroism (CD), isothermal titration calorimetry (ITC), surface plasma resonance (SPR), and quartz crystal microbalance (QCM), etc. SPR and QCM can qualitatively indicate with high sensitivity whether or not there exist interactions between NPs and proteins. ITC can monitor thermodynamics of the nanoparticle−protein interactions, revealing the dominating driving force of such interactions. CD can probe the conformational change of protein induced by interacting with the NP surfaces. There is no general method that is suitable for every system. Normally, several techniques have to be combined in order to obtain insight into the system of interest. The ideal method of choice should be noninvasive, in situ, sensitive and low-cost.[23] Some techniques, such as fluorescence based methodology, may fulfill part of these features.[26] Especially, polymeric nanoparticle based ratiometric fluorescent sensors have made significant progress via exploiting the Förster Resonance Energy Transfer (FRET) effect.[27−32] FRET is a distance-sensitive nonradiation energy transfer between two chromophores-the fluorescent receptor and donor.[33] Only when the distance of the two chromophores is blow 10 nm, FRET can occur. FRET also has many other advantages such as nanosecond time scale, simplicity of the experimental implementation and ability to work with dilute solutions. These precious features make FRET a popular and powerful tool in the investigation of protein−protein and protein−ligand interactions as well as sensitive biosensor.[34] Recently, S.W. Morton et al. demonstrated an elegant approach to real-time monitoring the serum stability and biodistribution of polymeric micellar systems in vivo utilizing the FRET as imaging modality.[35]

In the current work, we shall focus on the polymer nanoparticle−protein interface and develop a FRET based strategy to investigate the reversible and dynamic interactions of the two partners, in order to reveal the underpinning mechanism which can be further used to optimize the efficiency of the interactions between polymeric nanoparticles and proteins. For this, a well-controlled model system is needed. In our previous work, we have developed artificial chaperone based on nanoscale mixed shell polymeric micelles (MSPMs), which refer to polymeric micelles with at least two kinds of dissimilar polymer chains in the micellar shell.[36] We have demonstrated the pronounced competency of such MSPMs in preventing the heat denaturation of a wide spectrum of proteins and retarding the fibrillation of Alzheimer-disease relative amyloid beta proteins.[8,21] The mechanism is assumed to work through reversible catching and releasing of the unfolded protein intermediates by the micellar surface under appropriate conditions. Therefore, such well-controlled system can be exploited as a general model to test strategies for monitoring the reversible interactions of nanoparticles with proteins. Herein, we design a new kind of polymeric nanoparticles consisting of a poly(ethylene glycol)/poly(*N*-isopropylacrylamide) (PEG/PNIPAM) mixed shell. Induced by temperature stimuli, the constitute PNIPAM chain in the micellar shell can transform between a collapsed hydrophobic and extended hydrophilic state, which can conveniently realize reversible interaction with proteins (Scheme 1).[37] Most importantly, appropriate chemistry is exploited to place the FRET acceptors precisely at specific locations. Thermoresponsive interactions of such model micelles with a FITC donor labeled protein - FITC-lysozyme, will be monitored by the FRET technique. Some unexpected insights are revealed, which will help us optimize our future design of polymer based chaperones with enhanced properties.

Scheme 1. Schematic Illustration of the Reversible and Dynamic Interactions between MSPMs and the Substrate Proteins during Heating/Cooling Cycle[a]

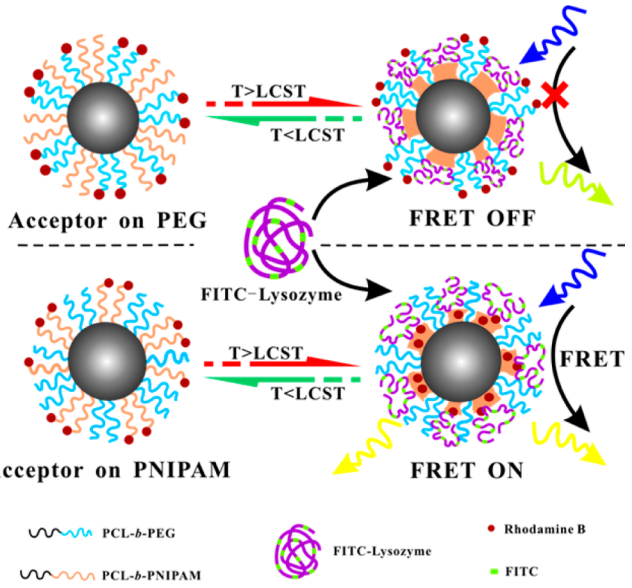

[a]The protein is labeled with FITC as the FRET donor and MSPMs are labeled with rhodamine B hydrazide as the FRET acceptors. Different FRET phenomena can be observed when the fluorescent acceptors are located at different polymer segments.

2. EXPERIMENTAL SECTION

2.1. Materials. All chemicals are obtained from Sigma-Aldrich unless otherwise noted. 2, 2′-Azoisobutyronitrile (AIBN) was recrystallized from ethanol twice and dried under vacuum. *N*-isopropylacrylamide (NIPAM) from TCI was recrystallized from hexane and dried under vacuum. ε-Caprolactone from Alfa was distilled under reduced pressure before use. Methoxypoly(ethylene glycol) (CH_3O-PEG_{113}-OH) (M_n = 5000 and the polydispersity index (PDI) = 1.05) was dried under vacuum. *t*-Boc-NH-PEG−OH with M_n = 5000 and PDI = 1.08 was obtained from Shanghai Yare Biotech. (Shanhai, China) and dried under vacuum. *S*-1-Dodecyl-*S*′-(α,α′-dimethyl-α″-acetic acid) trithiocarbonate (TTC) was purchased from Changzhou Yipingtang (Changzhou, China). Stannous octoate ($Sn(Oct)_2$, from Alfa), fluorescein isothiocyanate (FITC), rhodamine B and chicken egg white lysozyme (referred as lysozyme) were used without further purification. All the organic solvents were dried following the standard procedure.

2.2. Synthesis of the Block Copolymers. The details for the synthesis and characterization of the two polymers, poly(ε-caprolactone)-*block*-(ethylene glycol) (PCL-*b*-PEG) and PCL-NH_2,

DOI: 10.1021/acsami.5b00684
ACS Appl. Mater. Interfaces 2015, 7, 10238−10249

Scheme 2. Synthesis of Poly(ε-Caprolactone)-*block*-poly(*N*-isopropylacrylamide) (PCL-*b*-PNIPAM) (A) and Poly(ε-Caprolactone)-*block*-poly(ethylene glycol) (PCL-*b*-PEG) (B) Labeled with Rhodamine B Hydrazide at the End of the PNIPAM and PEG Block, Respectively

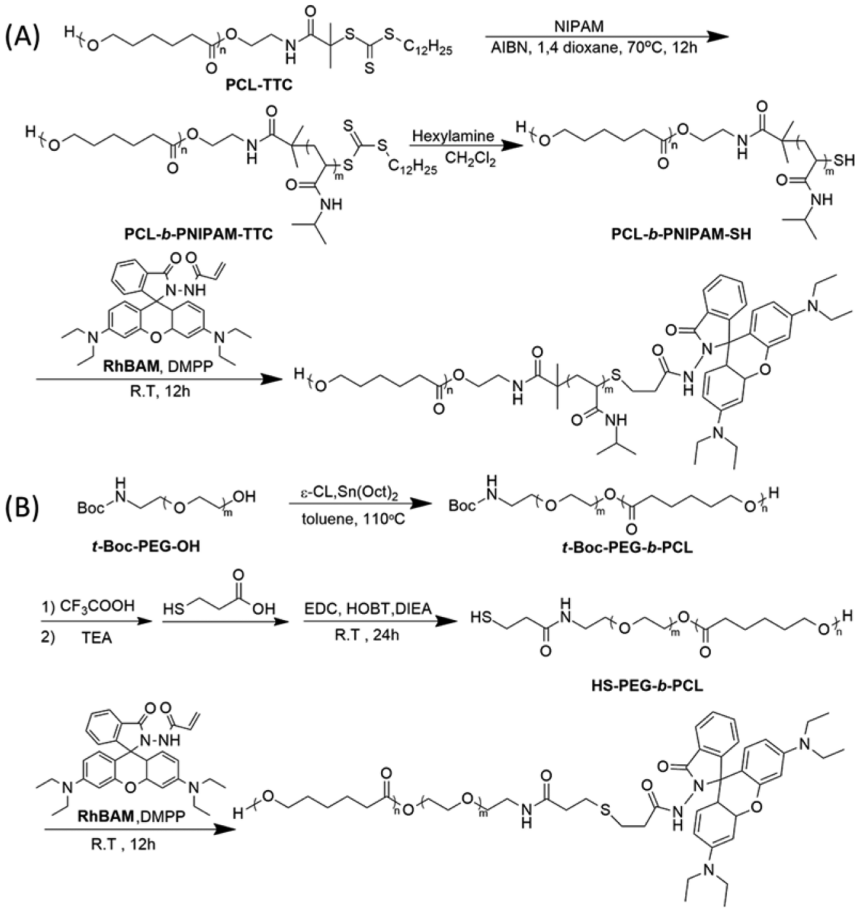

have been reported by our group,[38] and is also summarized in the Supporting Information (Scheme S1). Herein, we only describe the procedure for the synthesis of PCL-*b*-PEG and PCL-*b*-PNIPAM that are labeled with rhodamine B hydrazide (RhBAM) at the end of either PEG or PNIPAM through the thiol−ene click reaction (Scheme 2).

2.2.1. Synthesis of RhBAM Terminated Block Polymer PCL-b-PNIPAM (PCL_{83}-b-$PNIPAM_{90}$-RhBAM). The synthetic process was illustrated in Scheme 2. First, acryloyl rhodamine B hydrazide (RhBAM) was synthesized according to refs 39 and 28 (Scheme S1A in the Supporting Information). PCL_{83}-*b*-$PNIAM_{90}$ was synthesized by reversible addition−fragmentation chain transfer (RAFT) polymerization, using PCL labeled with a trithiocarbonate (TTC) group (PCL-TTC) as the chain transfer agent and AIBN as the initiator (Scheme 2A and Supporting Information Scheme S1C). Briefly, PCL-TTC (0.22 g, 0.022 mmol), NIPAM (0.22 g, 1.91 mmol), and AIBN (1.18 mg, 0.0072 mmol) were added into the reaction flask and then 4 mL of 1,4 dioxane was added. After three freeze-degas-thaw cycles, polymerization was conducted at 70 °C for 12 h. The mixture was diluted with THF and then precipitated into excess diethyl ether. The precipitate was dried under vacuum. To synthesize the RhBAM terminated PCL_{83}-*b*-$PNIAM_{90}$, a mixture of 0.5 g PCL-*b*-PNIPAM, 130 mg RhBAM, 35 μL dimethylphenylphosphine (DMPP) and 10 mL dichloromethane were added into a 50 mL round bottomed flask. The solution was deoxygenated by N_2 for 20 min, and then 2.5 mL of hexylamine was added via a 5 mL syringe. The mixture was purged with N_2 for another 15 min, and then stirred overnight at room temperature in dark. The mixture was diluted with CH_2Cl_2 and poured into excess amount of chilled diethyl ether. The precipitate was dried under vacuum. In the following text, the RhBAM terminated block polymer PCL_{83}-*b*-$PNIPAM_{90}$ will be referred as PCL_{83}-*b*-$PNIAM_{90}$-RhBAM. The subscripts in the bock copolymer denote the degrees of polymerization.

2.2.2. Synthesis of RhBAM Terminated Block Polymer PCL-b-PEG (PCL-b-PEG-RhBAM). The block copolymer *t*-Boc-PEG-*b*-PCL was synthesized by ring opening polymerization (ROP) of ε-caprolactone using *t*-Boc-PEG-OH as the initiator and $Sn(Oct)_2$ as the catalyst in toluene (Scheme 2B). Briefly, *t*-Boc-PEG−OH (0.5 g, 0.1 mmol), ε-caprolactone (1 g, 8.76 mmol), and two drops of $Sn(Oct)_2$ were mixed in a reaction flask and then 5 mL of toluene was added. The polymerization was conducted at 110 °C for 12 h. The reaction mixture was diluted with dichloromethane and then precipitated into excess amount of chilled diethyl ether. The removal of the Boc group was performed in the mixing solvent of trifluoroacetic acid and dichloromethane (1/1, v/v) at room temperature for 24 h, and then the mixture was precipitated into large amount of diethyl ether. The precipitate was treated in the mixing solvent of triethylamine (TEA) and dichloromethane (1/1, v/v) at room temperature for 24 h. The mixture was precipitated into excess diethyl ether and dried under vacuum, resulting in H_2N-PEG-*b*-PCL. To obtain the thiol-terminated block copolymer (HS-PEG-*b*-PCL), H_2N-PEG-*b*-PCL (0.85 g, 0.05 mmol), 3-mercaptopropionic acid (53.07 mg, 0.5 mmol), 1-(3-(dimethylamino)propyl)-3-ethylcarbodiimide hydrochloride (95.85 mg, 0.5 mmol), *N*,*N*-diisopropylethylamine (65 mg, 0.5 mmol), and 1-hydroxybeznzotriazole (68 mg, 0.5 mmol) were dissolved in 4 mL dichloromethane. The mixture was stirred for 24 h at room temperature and then poured into excess chilled diethyl ether. The precipitate was dried under vacuum. HS-PEG-*b*-PCL was then labeled with RhBAM following the same procedure of PCL_{88}-*b*-$PNIPAM_{90}$-RhBAM.

DOI: 10.1021/acsami.5b00684
ACS Appl. Mater. Interfaces 2015, 7, 10238−10249

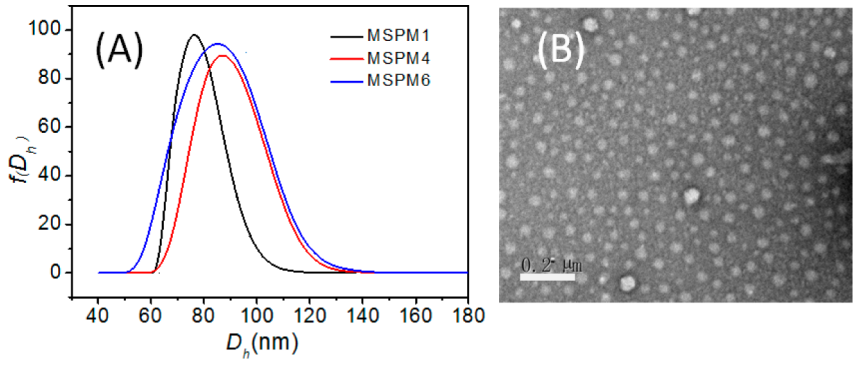

Figure 1. Hydrodynamic size distribution measured by dynamic light scattering (A) and TEM photo of mixed shell polymeric micelles with a PEG: PNIPAM ratio in the shell of 1:6 (B). MSPM1, MSPM4, and MSPM6 refer to mixed shell polymeric micelles with a PEG: PNIPAM mass ratio in the shell of 1:1, 1:4 and 1:6, respectively.

2.3. Preparation of Mixed Shell Polymeric Micelles. First, different amount of block copolymers PCL-*b*-PEG and PCL-*b*-PNIPAM with or without RhBAM at the end of PEG or PNIPAM were dissolved in a given volume of acetone. Subsequently, the polymer solution was added dropwise into a given amount of distilled water under vigorous stirring until the opalescence appeared, indicating the formation of micelles. The solution was further stirred overnight and dialyzed against water to remove acetone. The final concentration of the micelles was 0.67 mg mL^{-1}.

2.4. FITC Labeling of Lysozyme. Labeling of lysozyme with FITC was performed as described previously.[40] Briefly, 20 mg lysozyme was dissolved in 3 mL 0.1 M borate buffer (pH 9.0) and 1 mg FITC was dissolved in 1 mL DMF. The FITC solution was added dropwise into the solution of lysozyme. Finally, the mixture was incubated overnight at 4 °C and then dialyzed against PBS (10 mM, pH = 7.6) and acetate buffer (10 mM, pH = 5.5) to remove unreacted FITC. The concentration of the stock solution of FITC labeled lysozyme was 9.14 mg mL^{-1} measured by UV−vis. As for the number of FTIC per protein, 2−3 FITC per lysozyme was estimated following literature.[41] In the following text, FITC labeled lysozyme will be referred as FITC-lysozyme.

2.5. FRET experiment. Liu and his co-workers reported that the RhBAM moiety is in the spirolactam form above pH = 6 which is nonfluorescent; whereas below pH = 6, it transforms into the acyclic form and emits strong fluorescence.[28] So the FRET experiments were conducted in buffers at pH = 5.5. The stock solution of FITC-lysozyme was diluted 1000 times before it was used in the FRET experiment. Briefly, 1 mL micelle suspension and 200 μL diluted FITC-lysozyme solution were mixed together. The FRET or fluorescent measurements were performed on a Hitachi F-4600 spectrofluorometer equipped with a thermostated cell holder. The temperature of the holder was controlled with an accuracy of 0.01 °C by an HAAKE A28 external circulating water bath installed with an HAAKE SC 100 controller (Thermo Scientific). The fluorescence emission spectra in the range of 500 to 700 nm were recorded under various conditions with an excitation wavelength at 450 nm. The excitation and emission slit widths were 5 and 10 nm, respectively.

2.6. Heat denaturation of FITC-lysozyme and enzymatic activity assay. Lysozyme with or without FITC labeling was subjected to steady state heating in the presence or absence of polymeric micelles. Incubation of lysozyme at 70 °C for 30 min is enough to induce denaturation.[42,43] Subsequent refolding process was carried out by cooling and storing the mixture in a refrigerator at 4 °C. The enzymatic activity of the cooled lysozyme was then assessed following a published procedure with some modifications.[8,44] *Micrococcus lysodeikticus* cell suspension (420 μL 0.3 mg mL^{-1}) was added to 80 μL lysozyme solution (0.1 mg mL^{-1}), under vigorously shaking. The light scattering intensity of the solution, which is directly proportional to the amount of active lysozyme in the sample, was then measured by monitoring the apparent absorbance at 450 nm. The sodium phosphate buffer (66 mM, pH 6.2) was used to prepare the *Micrococcus lysodeikticus* cell suspension and lysozyme solution.

2.7. Characterization. ^{1}H nuclear magnetic resonance (^{1}H NMR) spectra were obtained on a Varian UNITY-plus 400 M nuclear magnetic resonance spectrometer at room temperature using $CDCl_3$ as solvents. The number-average molecular weight (M_n), weight-average molecular weight (M_w) and polydispersity (M_w/M_n) of the block polymers were determined by gel permeation chromatograph (GPC) at 35 °C on a Waters 1525 chromatograph equipped with a Waters 2414 refractive index detector. THF was used as eluent at a flow rate of 1 mL min^{-1}. Polystyrene standards were employed for calibration. Dynamic light scattering (DLS) measurements were performed on a laser light scattering spectrometer (BI-200SM) equipped with a digital correlator (BI-9000AT) at 636 nm at given temperatures. The zeta potential values were measured on a Brookheaven ZetaPALS (Brookheaven Instrument, USA) at given temperature. All the samples were obtained by filtering through a 0.45 μm Millipore filter. X-ray photoelectron spectroscopy (XPS) measurements were performed with a Kratos Axis Ultra DLD multitechnique X-ray photoelectron spectroscopy (Kratos Analytical Ltd., UK). Transmission electron microscopy (TEM) measurements were performed using a Philips T20ST electron microscope at an acceleration voltage of 100 kV. The TEM samples were negative stained by 2% uranyl acetate solution. UV−vis absorption spectra were measured on a UV-2550 UV−vis spectrophotometer (Shimadzu, Japan).

3. RESULTS AND DISCUSSION

3.1. Preparation of Model Mixed Shell Polymeric Micelles with FRET acceptors. To prepare model mixed shell polymeric micelles (MSPMs) with the FRET acceptor placed at specific locations, poly(ε-caprolactone)-*block*-(ethylene glycol) (PCL-*b*-PEG) and poly(ε-caprolactone)-*block*-poly(*N*-isopropylacrylamide) (PCL-*b*-PNIPAM), with or without rhodamine B hydrazide at the end of either the PEG or PNIPAM block, are synthesized (Scheme 2 and Supporting Information Scheme S1). PCL_{78}-*b*-PEG_{113} is obtained by ring-opening polymerization (ROP) of ε-caprolactone using PEG-OH as the initiator (Supporting Information Scheme S1). To locally place rhodamine B hydrazide at the end of the PEG block of the PCL-*b*-PEG (PCL-*b*-PEG-RhBAM), a thiol group is introduced to the end of the PEG block and then coupled with acrylyl rhodamine B hydrazide (RhBAM) via the thiol−ene click reaction (Scheme 2B).[45] PCL_{83}-*b*-$PNIPAM_{90}$ is synthesized by reversible addition−fragmentation chain transfer (RAFT) polymerization, using thiocarbonylthio terminated PCL as the macro chain transfer agent (Scheme 2A). The thiocarbonylthio end-group is cleaved into the thiol group which is then coupled with RhBAM, resulting in PCL-*b*-

DOI: 10.1021/acsami.5b00684
ACS Appl. Mater. Interfaces 2015, 7, 10238−10249

PNIPAM-RhBAM with RhBAM at the end of the PNIPAM block. Characterization of the block polymers is listed in the Supporting Information. The ^{1}H NMR spectra clearly indicate that the fluorescent acceptor is successfully labeled to the end of the respective blocks.

The mixed shell polymeric micelles (MSPMs) consist of a PCL core and a mixed PEG/PNIPAM shell are prepared by self-coassembly of PCL-*b*-PEG (-RhBAM) and PCL-*b*-PNIPAM (-RhBAM) in aqueous solution (Scheme 1).[46] Combination of the different block copolymers offers a flexible means to prepare micelles with varied surface properties. For instance, the ratio of PEG/PNIPAM in the shell can be adjusted by controlling the mass ratio of the starting block polymers. Especially valuable to the current work, the fluorescent acceptor can be precisely placed to the end of either the PEG or PNIPAM block of the final micelles. The size distribution of the as-prepared MSPMs is monitored by dynamic light scattering (DLS) (Figure 1A). All of the micelles with varied PEG/PNIPAM mass ratio in the shell have a narrow size distribution and the average hydrodynamic diameter centers around 80 nm. Negative staining TEM indicates each kind of MSPMs has a spherical shape and the size matches the diameters measured by DLS (Figure 1B and Supporting Information Figure S4). Simple micelles with only PEG or PNIPAM in the shell are also prepared. The zeta-potentials of the different micelle formulations in the acetate buffer (pH 5.5) have slightly negative values and show no pronounced variation upon heating (Supporting Information Table S1). The surface chemical composition of the mixed micelles is confirmed by X-ray photoelectron spectroscopy (XPS) (Figure S3). Upon labeling of RhBAM, the O 1s peak at 531.6 eV slightly shifts to a higher binding energy (BE) with increased intensity than the PCL-*b*-PNIPAM-TTC MSPMs, indicating that the fluorescent acceptors RhBAM are directly labeled at the end of PNIPAM segments (Supporting Information Figure S3B). In the case of MSPMs consisting of PCL-*b*-PEG and PCL-*b*-PNIPAM-TTC in which the thiocarbonylthio group from the RAFT polymerization sitting at the end of the PNIPAM blocks, the characteristic S 2p peak divides into two peaks locating at 163.2 and 168.6 eV, due to the two different states of sulfur (C═S and C−S,) existing in the thiocarbonylthio group (Supporting Information Figure S3C). In contrast, there is only one S 2p peak at 169 eV in the case of MSPMs consisting of PCL-*b*-PEG and PCL-*b*-PNIPAM-RhBAM, in which only the single state of the carbon−sulfur bond (C−S) exists. In addition, UV−vis absorbance spectra of simple micelles consisting of either PCL-*b*-PNIPAM before and after RhBAM labeling through thiol−ene click reaction is also measured and listed in Supporting Information Figure S2. As the thiocarbonylthio groups are cleaved into thiol groups and then react with the double bond of RhBAM, the trithiocarbonate absorbance at 310 nm disappears from the UV spectrum of the simple micelles consisting of PCL-*b*-PNIPAM-RhBAM. This means the trithiocarbonate are successfully reduced into thiol groups and the high efficient thiol−ene click reaction is perfectly performed. So almost all the terminal of PNIPAM segments are linked with RhBAM after the click reaction. In summary, these results clearly indicate that MSPMs are decorated with the FRET acceptor-RhBAM at their outmost surface.

3.2. Effect of Acceptor-Labeled MSPMs on the Prevention of Thermal Denaturation of Lysozyme. FITC-labeled lysozyme (FITC-lysozyme) has been widely used as a model protein to investigate its interaction with many substrates and surfaces.[7,20] It is well established that the FITC labeling has no effect on its tertiary structure and enzymatic activity.[40,41] Micelles with an identical mixed shell while containing no labeled dyes have exhibited excellent effects on the prevention of thermal denaturation of pristine lysozyme.[8] To demonstrate the above micelles bearing the fluorescent acceptors have similar effects on FITC-lysozyme, the relative enzymatic activity of FITC-lysozyme after heat treatment in the presence of or absence of acceptor-labeled MSPMs at various locations are investigated, following the method reported previously by our group (Figure 2).[8] Slightly different from

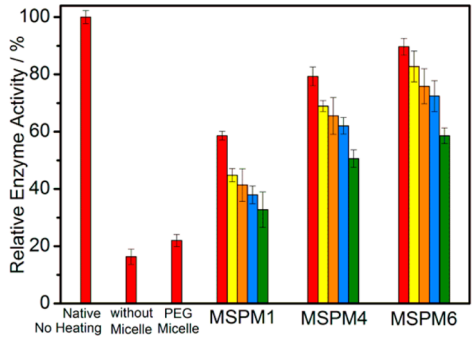

Figure 2. Residual enzyme activity of FITC-lysozyme measured at room temperature after cooling from the heat treatment at 70 °C for 30 min in the absence or presence of polymeric micelles. PEG micelles refer to micelles consisting of only PCL-*b*-PEG. In the case of each MSPM, the bars from left to right represent MSPM with continuous dilutions based on the original micelle suspension (from red to green). The meaning of MSPM1, MSPM4, and MSPM6 is the same as Figure 1.

previous work, the FRET experiment has to be performed under conditions with pH = 5.5, since the FRET acceptor-RhBAM moiety is in the spirolactam form above pH = 6 which is nonfluorescent; whereas below pH = 6, it transforms into the acyclic form and emits strong fluorescence.[28] Therefore, the stability and heating induced denaturation of FITC-lysozyme alone is investigated under the conditions suitable for the following FRET experiments (pH = 5.5), to exclude potential influence of the pH variation. At pH = 5.5, lysozyme adopts α-helical dominated conformation with two negative bands around 208 and 222 nm in the CD spectrum, which are identical to that of the same protein at physiological pH (pH 7.5, Supporting Information Figure S5A). During heating up to 50 °C, there is no change in the CD spectrum while a sharp decrease of intensity occurs to 208 nm at 70 °C, suggesting that the fractions of α-helical structure decreases while that of β-sheet increases because of the unfolding of the protein.[47] When FITC-lysozyme alone is heated from room temperature to 70 °C and kept at this temperature for 30 min, only 16% enzymatic activity is remained after cooling back to room temperature (Figure 2), indicating that incubation at 70 °C is enough to denaturize the enzyme in the absence of any additives.[42,43,47,48] All of these results points to the fact that the structure and heating denaturation progress are the same for lysozyme at 5.5 and physiological pH value.

If FITC-lysozyme is subjected to the same heat treatment in the presence of PCL-*b*-PEG single micelles that do not have the PCL-*b*-PNIPAM component, only 25% enzymatic activity is remained (Figure 2). However, the protein could remain as

DOI: 10.1021/acsami.5b00684
ACS Appl. Mater. Interfaces 2015, 7, 10238−10249

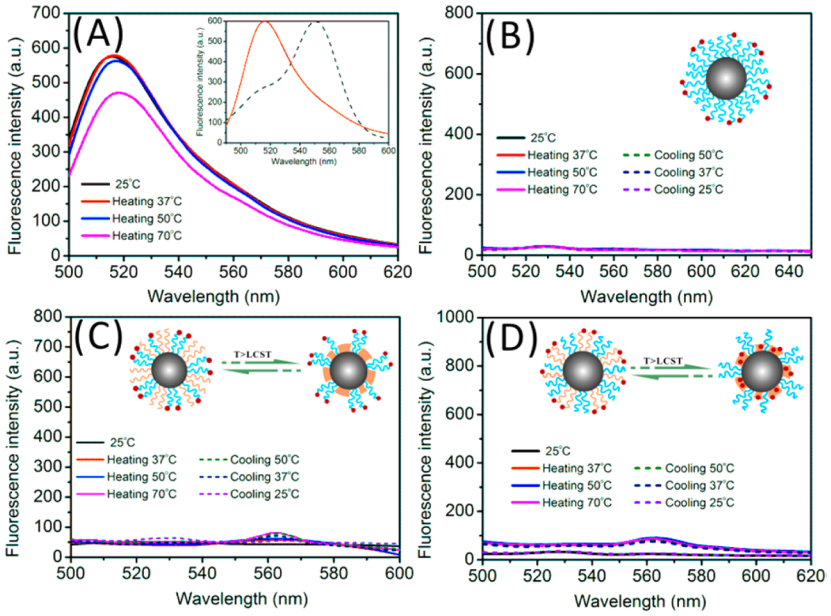

Figure 3. Fluorescence emission behavior of FITC-lysozyme and RhBAM labeled polymeric micelles when being excited at 450 nm, respectively. (A) Spectra of FITC-lysozyme at various temperatures when being excited at 450 nm (solid lines). Inset: The sold line is the fluorescence emission of FITC-lysozyme at 25 °C while the dashed line is the absorbance spectra of MSPMs labeled with RhBAM at the end of the PNIPAM chain. Panels B–D are spectra of the simple micelle or MSPMs with RhBAM labeled at various locations. Panel B shows the simple micelle consisting of only PEG, at the end of which RhBAM is labeled. Panel C shows MSPMs with a 1:6 PEG/PNIPAM shell. The acceptors are labeled at the end of the PEG chain. Panel D shows the spectra of MSPMs with a 1:6 PEG/PNIPAM shell and the acceptors are labeled at the end of the PNIPAM chain.

high as 90% activities in the presence of acceptor-labeled MSPMs. The efficacy of the MSPM on the thermal stability of lysozyme is dependent on the ratio of PEG/PNIPAM in the shell and the relative amount of the micelles to the enzyme (Figure 2). The general tendency is that increasing PNIPAM content in the shell of MSPMs leads to increasing remained enzyme activity. If lowering the relative amount of the micelles to the enzyme by dilution, the remained enzyme activity also decreases. Take the MSPM6 as an example, the residual enzyme activity is 90% when the concentration of the micelles is 0.67 mg mL^{-1} and decrease to 58% when the concentration of the micelle was decrease to 0.14 mg mL^{-1} by dilution (from the red to green column labeled with MSPM6 see in Figure 2). All of these results are consistent with our previous observation on the similar system.[8] Therefore, decoration of fluorescent acceptors onto the surface of the micelles does not influence the capability of the current micelles to prevent the thermo-denaturation of lysozyme. As assumed in our previous work and also by others,[7,8] the key step is to prevent irreversible aggregation of (unfolded) lysozyme by trapping the unfolded intermediates with exposed hydrophobic sites of lysozyme to the hydrophobic PNIPAM domains formed during heating. Upon cooling, release and refolding of the trapped intermediates occur (Scheme 1).

3.3. FRET between Acceptor-Labeled MSPMs and FITC-Labeled Lysozyme. Interactions between FITC-lysozyme and RhBAM-labeled MSPMs during heat treatments are assumed to follow the procedure as illustrated in Scheme 1. If so, adsorption of (unfolded) FITC-labeled lysozyme to the micellar surface with acceptors should bring the classical FRET pair-FITC and rhodamine B in the close proximity with a distance enough to trigger the FRET effect. To investigate such effect and gain further insight into the detailed mechanism of the adsorption of lysozyme onto the surface of micelles, three kinds of micelles are designed, which have the fluoresce acceptor, that is, rhodamine B hydrazide (RhBAM), sitting at various locations (insets of Figure 3). The fluorescent emission behavior of FITC-lysozyme in the presence of such MSPMs is investigated at the characteristic excitation wavelength of FITC (450 nm). Before this, the fluorescent emission behavior of FITC-lysozyme and the RhBAM-labeled simple micelles or MSPMs are first checked separately under the same conditions (Figure 3 and see Supporting Information). First of all, FITC-lysozyme shows a fluorescent emission peak at around 515 nm when being exited at 450 nm while the absorption maxima of RhBAM-labeled micelles locates around 550 nm (inset in Figure 3).[49] The emission spectra of FITC-lysozyme has a large overlap with the absorption spectra of RhBAM-labeled micelles (Figure 3A), which fulfills the requirement of effective FRET effects (from FITC to RhBAM). Upon heating up to 50 °C, the emission behavior of FITC-lysozyme alone has no any change (Figure 3A). At 70 °C, a sharp decrease occurs to the emission intensity at 515 nm, the characteristic emission maxima of FITC. Such phenomena are due to the unfolding and aggregation of the lysozyme, which change the local environment of FITC moieties. When exciting RhBAM labeled MSPMs or simple micelles at 450 nm in the absence of any FITC-lysozyme, the emission in the range of 500–700 nm during heating and cooling, especially the characteristic emission maxima of RhBAM at 562 nm is very weak in the whole temperature range of interest (Figure 3B–D and Figures S6 and S7 in Supporting Information). The very weak emission peaks around 560 nm in the cases of MSPMs during the heating/cooling procedure can be ascribed to the cross-talk effect of FRET which is probably originated from the leakage of the donor fluorescence into the detection channel for the acceptor fluorescence.[50] The influence of the cross-talk effect can be corrected by subtracting the background (the fluorescence emission spectra of RhBAM-Micelles excited at 450 nm) in the following FRET experiments.[51] Therefore, any

DOI: 10.1021/acsami.5b00684
ACS Appl. Mater. Interfaces 2015, 7, 10238–10249

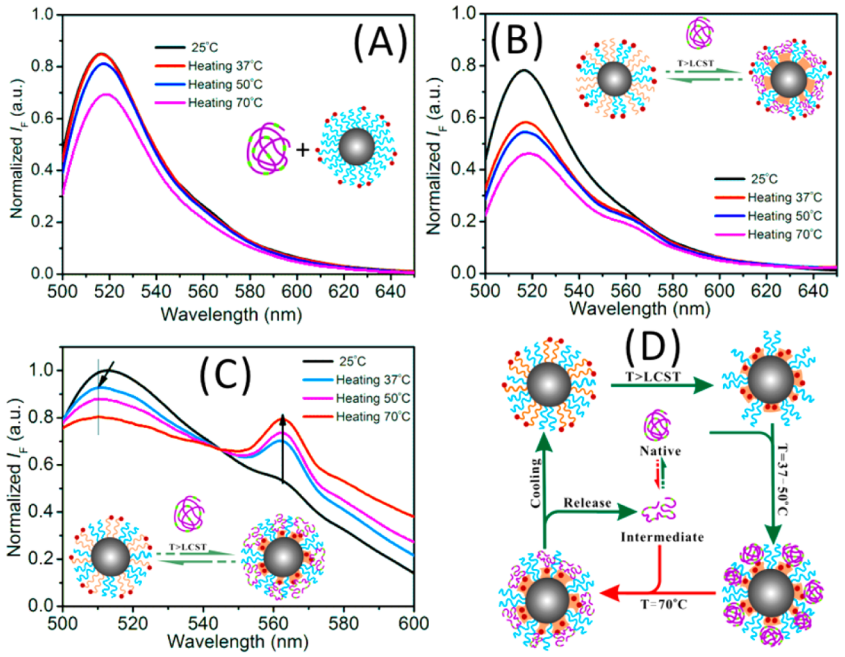

Figure 4. Fluorescence emission spectra during heating in the mixture of FITC-labeled lysozyme (FITC-lysozyme) and simple micelles or mixed shell polymeric micelles (MSPMs) onto which the FRET acceptors are placed at various locations. The excitation was fixed at 450 nm, such that only FITC-lysozyme was directly excited. The emission was scanned from 450 to 800 nm. (A) Spectra of the mixture of FITC-lysozyme and simple micelles consisting of only PEG in the micellar shell. The FRET acceptor-RhBAM is labeled at the end of the PEG chain (Inset). No emission can be detected at 562 nm upon heating. (B) Spectra of the mixture of FITC-lysozyme and MSPMs with a 1:6 PEG/PNIPAM shell. The acceptors are labeled at the end of the PEG chain. (C) MSPMs with a 1:6 PEG/PNIPAM shell. The acceptors are labeled at the end of PNIPAM chain. (D) Schematic illustration of the new insight into the interaction of proteins with MSPMs upon heating and cooling.

pronounced emission at 562 nm should be due to the FRET effect. In summary, the current combination of MSPMs or single micelles decorated with FRET acceptors and FITC-lysozyme is an ideal pair for the following FRET investigations.

Listed in Figure 4 are the fluorescent emission behaviors of FITC-lysozyme in the presence of three kinds of polymeric micelles at the characteristic excitation wavelength of FITC (450 nm). At room temperature (RT), regardless of the location of the acceptor dyes in the micelles, the emission is dominated by FTIC-lysozyme at 515 nm and there is barely any emission at around 562 nm, the characteristic emission maxima of the "open" form of RhBAM under the current conditions where pH = 5.5. Therefore, there exists no interaction between lysozyme and the micelles of various surface properties. Such behavior is understandable since PEG is a classic sheath shell for nanoparticles to avoid random adsorption of proteins and we have also demonstrated the PEG/PNIPAM mixed shell even has improved performance in this regard.[6] Upon heating, difference in the fluorescent emission behavior of the three kinds of micelles is clearly distinguishable (Figure 4). In the case of simple micelles consisting of only PEG in the shell, no emission because of the FRET effect occurs at 562 nm upon heating from RT to 70 °C and incubating at this temperature (Figure 4A). The fluorescent emission spectra at various temperatures are identical to that of FITC-lysozyme in the absence of any micelles (Solid lines in Figure 3A). Therefore, there is no interaction between PEG single micelles and lysozyme even at the denaturation temperature of lysozyme. This is consistent with visible aggregation of lysozyme at 70 °C and the low recovered enzyme activity of the enzyme after cooling back in the presence of such kind of micelles (Figure 2). For the MSPMs with the acceptor labeled at the end of the PEG chains (Figure 4B), a very weak shoulder peak appears at around 562 nm during heating. Such peak does not change during the whole heating procedure, suggesting negligible FRET effects. However, it is noted that the emission behavior at 515 nm due to FITC-lysozyme itself is different between the two kinds of micelles of Figure 4A and B. At temperature up to 50 °C, the decrease of the fluorescent intensity at 515 nm is negligible in the case of the mixture of FITC-lysozyme and simple micelles only consisting of PEG in the shell (Figure 4A). Clear intensity decrease only occurs at 70 °C, due to the unfolding and aggregation of FITC-lysozyme at this temperature, which changes the local environments of FITC and interdye distance. In contrast, in the case of the MSPM of Figure 4B, significant decrease of the intensity can already be observed at 37 °C, followed by moderate decrease upon further heating. This behavior points to the fact that, although still in its native state, FITC-lysozyme probably already starts to be adsorbed onto the hydrophobic PNIPAM domains at 37 °C. Therefore, local environments of FITC are already changed at 37 °C, resulting in decreasing emission intensity. This speculation will be confirmed in the following discussion.

The fluorescent emission behavior of MSPMs with the acceptor labeled at the end of PNIPAM chains is unique among the three kinds of micelles (Figure 4C). Pronounced fluorescent emission increase of the intensity at the 562 nm due to the acceptor are observed during heating, concomitantly accompanied by decreasing intensity at 515 nm due to the donor. For this kind of micelles, the FRET acceptor should sit in the collapsed layers of PNIPAM when $T > T_{LCST}$ (Inset of Figure 4C). The FRET pair of the FITC and Rhodamine B has a characteristic FRET distance (R_0) of 5 nm.[52] Therefore, the

DOI: 10.1021/acsami.5b00684
ACS Appl. Mater. Interfaces 2015, 7, 10238−10249

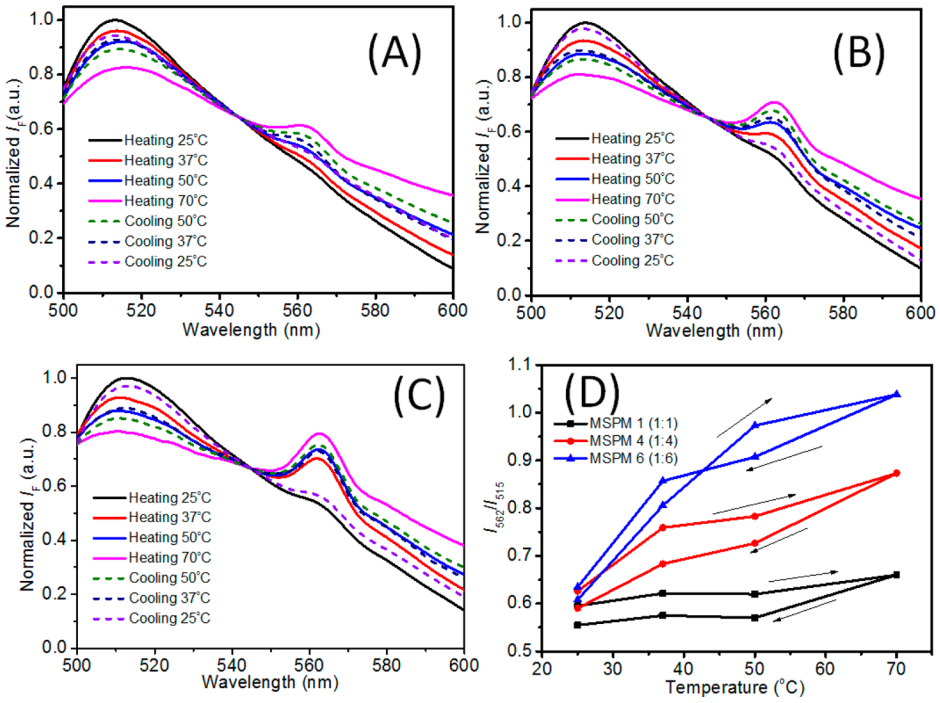

Figure 5. Reversibly of the adsorption and release of lysozyme onto the surface of mixed shell polymeric micelles as revealed by FRET. (A) MSPM1, (B) MSPM4, (C) MSPM6. (D) FRET ratio (I_{562}/I_{515}) versus temperature, as extracted from panels A−C. The meaning of MSPM1, MSPM4, and MSPM6 is the same as Figure 1.

clear FRET effect confirms the general assumption that lysozyme is brought to the close proximity of the hydrophobic PNIPAM domains during heating. Further investigation of Figure 4C reveals that pronounced FRET occurs already at 37 °C, at which PNIPAM chains collapse onto the micellar core to form hydrophobic domains while lysozyme is still in its native state. The FRET effect is only moderately enhanced by further heating to 70 °C, at which lysozyme starts to denaturate. This phenomenon is exactly consistent with the sharp decrease of the fluorescent emission of FITC at 37 °C in the case of MSPMs with the acceptor labeled at the end of the PEG chains (Figure 4B), as discussed above. The clear FRET effect at 37 °C suggests the close proximity of lysozyme to the hydrophobic surface which could be considered as adsorption since the FRET distance, R_0, of the current fluorescent pair is less than 5 nm.[52] Adsorption of native lysozyme to hydrophobic PNIPAM domains has also been observed by many others.[7,20] Shea et al. has found more than 50% lysozyme are adsorbed onto the surface of their polymeric nanoparticles with PNIPAM components at 40 °C.[7] Based on these observations, we suggest herein the following revised mechanism of our MSPMs to prevent thermal denaturation of lysozyme (Figure 4D). At first, native lysozyme is adsorbed onto the hydrophobic PNIPAM domains as soon as the temperature approaches the LCST of PNIPAM chains. During further heating to the denaturation temperature, lysozyme will unfold to expose its hydrophobic core, which might further enhance the interaction of lysozyme with the hydrophobic PNIPAM domains. Most importantly, by preadsorbed onto the PNIPAM domain, heat-triggered irreversible aggregation of unfolded lysozyme is largely avoided. During cooling, the transformation PNIPAM domains from the hydrophobic to hydrophilic state will release segregated unfolded lysozyme, during which, refolding into the native state will occur.[7]

Although the fluorescent emission behaviors of the two kinds of micelles in Figure 4B and 4C both origin from the same protein-micelle interaction, the FRET in the former is negligible while dominant in the latter. Both kinds of micelles have identical structure and similar effects on preventing the thermal denaturation of FITC-lysozyme, through adsorption of (unfolded) lysozyme intermediates to the collapsed PNIPAM hydrophobic domains. The only difference between the two kinds of micelles, after the PINPAM collapsed at $T > T_{LCST}$ of PNIPAM (32 °C), is that the FRET acceptors locate at the end of extended PEG chains for the former while they are sitting in the collapsed layers of PNIPAM for the latter (Insets in Figure 4B and C). The negligible FRET effect during heating the mixture of FITC-lysozyme and MSMPs in Figure 4B can be rationalized as follows: FITC-lysozyme or unfolded intermediates bind with the PNIPAM hydrophobic domains in such way that the FTIC moieties containing part of lysozyme are facing the PNIPAM domains and are shielded from Rhodamine B at the end of PEG. This scenario is similar to the reorientation of lysozyme to maximize its interaction with a macroscopic surface.[41] If we assume that the PEG chains in the micellar shell are in the brush region, PEG chains with a M_W of 5k have been suggested to correspond to a shell with a hydrodynamic thickness of more than 10 nm by Gref et al.[53] Therefore, the distance of FITC and Rhodamine B might be out of the effective range for the FRET effect. Upon heating, FITC-lysozyme approaches the collapsed hydrophobic PNIPAM domains through the extended PEG layer without interacting with the PEG chains. The collapse of the PNIPAM chains into the micellar core probably leaves behind cavity-like structure surrounding by stretched PEG chains, into which, (unfolded) proteins can be accommodated.

3.4. Reversibility of the Adsorption and Deadsorption during the Interaction of Lysozyme with MSPM. A key assumption in the prevention of heat denaturation of proteins

DOI: 10.1021/acsami.5b00684
ACS Appl. Mater. Interfaces 2015, 7, 10238−10249

by our MSPM based system is the reversible adsorption of proteins onto the hydrophobic domains of MSPMs under denaturation conditions (Scheme 1). The adsorbed unfolded intermediates can be released upon cooling. To investigate such reversible adsorption and deadsorption procedure, the FRET effect of the mixture of FITC-lysozyme and RhBAM-labeled MSPMs during heating and cooling are monitored (Figure 5). Upon heating, the FRET effect is observed with all of the three kinds of MSPMs with varied PEG/PNIPAM ratio in the shell. By cooling, during which lysozyme is expected to release from the surface of the MSPMs, the emission intensity at 515 nm increases while the one at 562 nm decreases. Such unique inverted FRET effects should be due to the increasing distance between FITC-lysozyme and the surface of the micelles during cooling. Therefore, the adsorbed FITC-lysozymes clearly detach from the micellar surface during cooling. As summarized in Figure 5D, the FRET ratio (I_{562}/I_{515}) versus temperature exhibits reversibility upon heating and then cooling.

The current MSPM-based system has the potential for the reuse. To demonstrate such property, the mixture of FITC-lysozyme and RhBAM-MSPM6 is subjected to multiple rounds of heating to 70 °C and cooling back to 25 °C, during which the FRET effect are monitored. Listed in Figure 6 is I_{562}/I_{515}

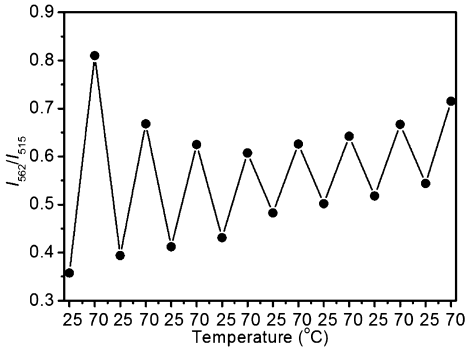

Figure 6. FRET ratio (I_{562}/I_{515}) of the mixture of FITC-lysozyme and RhBAM-MSPM6 when subjected to multiple rounds of heating to 70 °C and cooling back to 25 °C.

during the heating−cooling cycles. Although the I_{562}/I_{515} values are not constant during the cycling, reversible on−off switch like effects can be kept up to seven repeated heating−cooling cycles. Around 40% residual enzymatic activity can still be detected while lysozyme without any additives completely lost its enzymatic activity after the same round of heating and cooling. As also shown in Figure 6, the I_{562}/I_{515} value at 70 °C decreases at the first several rounds of heating and cooling while the ratio at 25 °C continually increases. Such phenomenon might be ascribed to the fact that some of lysozyme will stay on the micellar surface during cooling and the amount of the left-over will increase during increasing cycles of heating/cooling. Interprotein interactions between the left protein and the adsorbed ones during next heating might promote more protein adsorption. This is also explained the decreasing residual enzymatic activity during repeated heating−cooling cycles. From the heating/cooling cycles, it can be conclude that the enzyme in the presence of MSPMs can tolerant to several rounds of unexpected heating stress without losing all of the enzymatic activity. Such unique properties might be helpful to extend the shelf life of enzymes, especially under circumstances where the strict temperature control is not available.

3.5. Fast Dynamic Trapping of Lysozyme by MSPMs during Instant Heat Stress. During the above experiments, gradual heating and incubation at each temperature have been applied. Instant heat stress of proteins, during which the biomolecules are subjected to sudden heat stress is often encountered in practical applications. The current system can be also used to investigate such instance and to reveal the time scale of the adsorption of lysozyme to the hydrophobic domains of the micellar surface. For this purpose, the MSPM6 of the one in Figure 4C is preincubated at 70 °C, by which PNIPAM chains in the micellar shell collapse into hydrophobic domains and the micelles are turned into the active state. It is noted here that the micelles can still keep colloidal stability, thanks to the hydrophilic PEG brush. To the heated micelle suspension, FITC-lysozyme is added and the fluorescent emission behavior is recorded with an interval of 1 min (Figure 7). Initially, dominant fluorescent emission at 515 nm due to

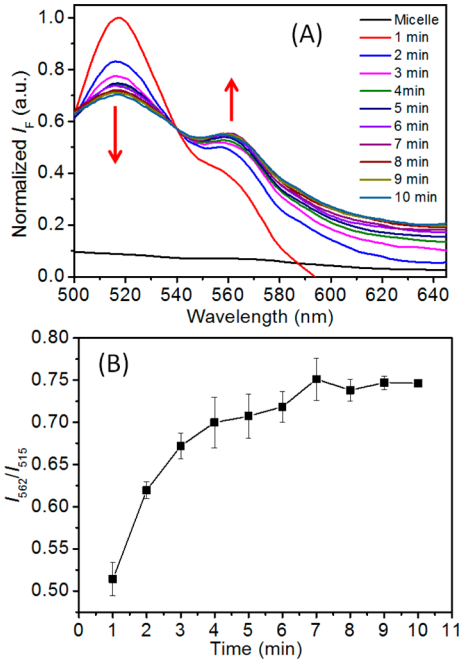

Figure 7. FRET effect when lysozyme is added directly into the MSPM6 suspension preincubated at temperature 70 °C (A). (B) FRET ratio (I_{562}/I_{515}) of the mixture of FITC-lysozyme and RhBAM-MSPM6.

FITC-lysozyme is observed, together with a shoulder peak at 562 nm. This shoulder peak then increases while the one at 515 nm decreases sharply. The ratio of emission intensity at 562 and 515 nm, I_{562}/I_{515}, versus time is listed in Figure 7B. I_{562}/I_{515} increases deeply right after adding the lysozyme and then level off after 4 min (Figure 7B). During the first 4 min, many events may occur, including unfolding of lysozyme due to the heat shock, adsorption of (unfolded) lysozyme onto the micellar surface, interprotein aggregations, etc. Since the FRET effect mainly probes the adsorption of (unfolded) lysozyme onto the micellar surface, the level-off of the I_{562}/I_{515} after 4 min suggest that such procedure is almost complete during that period.

3.6. Influence of Other Parameters on the Effect of MSPMs' Prohibition of the Heat Denaturation of Lysozyme. As observed in our previous work and also

DOI: 10.1021/acsami.5b00684
ACS Appl. Mater. Interfaces 2015, 7, 10238−10249

shown in Figure 2, the ratio of PEG/PNIPAM in the mixed shell of MSPMs and the relative amount of MSPMs to the enzyme have influence on the residual enzymatic activity of lysozyme after cooling back to room temperature in the presence of MSMPs.[8] These two parameters are also investigated here by comparing the FRET effect at temperature 70 °C (Figure 8). For MSPMs with the same concentration,

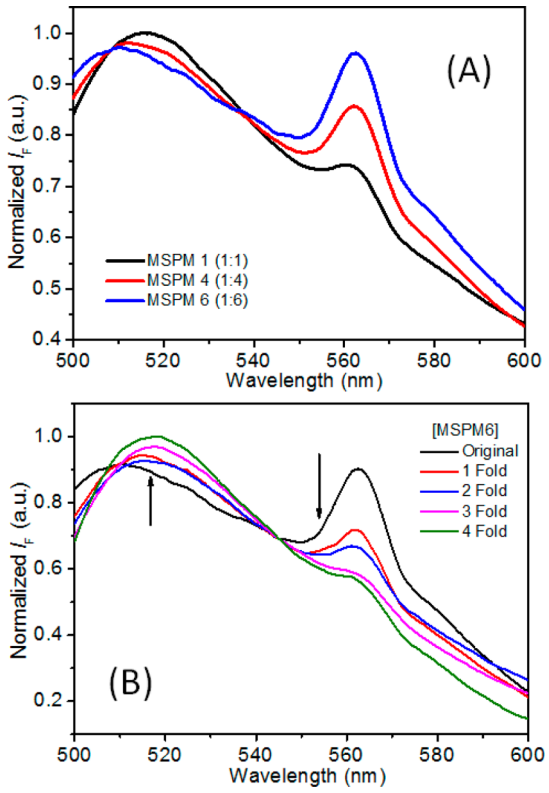

Figure 8. FRET effect at temperature 70 °C for MSPMs with different PEG/PNIPAM in the mixed shell (A) and for the MSPM6 with a defined PEG/PNIPAM ratio during dilution (B). The micelle concentration in (A) is the same for the three kinds of micelles. The original concentration of MSPM6 in (B) is 0.67 mg mL^{-1}.

higher PNIPAM/PEG ratio in the micellar shell leads to stronger FRET effects (Figure 8A), suggesting more FITC-lysozyme is adsorbed onto the surface of the MSPM. This phenomenon is in line with the fact that increasing the PNIPAM/PEG ratio results in increasing residual enzymatic activities (Figure 2). For the MSPM with a defined PEG/PNIPAM ratio, decreasing the relative amount of the MSPM to lysozyme by dilution the stock micelle suspension also results in decreasing FRET effects (Figure 8B and S8 in Supporting Information). In principle, both parameters presented in Figure 8 are to tune the PNIPAM domains available to (unfolded) lysozyme during denaturation. When the amount of lysozyme is constant, more PNIPAM domains means more lysozyme can be adsorbed onto the micellar surface and could be shielded from aggregation during the heat denaturation.

4. CONCLUSION

The current work focus on applying the Förster Resonance Energy Transfer (FRET) technique to investigate the interactions of our tailor-designed artificial chaperon based on mixed shell polymeric micelles (MSPMs) with their substrate proteins. Model MSPMs with FRET acceptors precisely placed at specific locations are prepared by self-coassembly of PCL-*b*-PEG and PCL-*b*-PNIPAM, with or without rhodamine B hydrazide at the end of either the PEG or PNIPAM block. Systematic investigations of the FRET effect of the mixture of FITC-lysozyme and the acceptor-bearing MSPMs upon heating confirm some aspects of our previous assumption but also reveal some valuable insights. All together, the micelles are in its dormant state and will not interfere with the functionality of the proteins. Upon heating above the LCST of PNIPAM, the micelles will transform into their functional states by holding the native proteins onto the hydrophobic PNIPAM domains well before approaching the denaturation condition. In this way, irreversible aggregation of unfolded protein intermediates, the main reason for thermal-denaturation of proteins can be suppressed during further heating. The FRET experiments also unambiguously confirm the reversible adsorption and releasing procedure of proteins with the micellar surface during heating/cooling cycles which can go up to several rounds. This work demonstrates that the FRET technique is well suitable for the study of polymeric particles with proteins if proper chemistry can be found to install the NPs and target protein with the FRET fluorophore pairs.

■ ASSOCIATED CONTENT

Supporting Information

The synthetic routes and characterization of block copolymers, TEM photo of MSPMs of other PEG/PNIPAM ratio, fluorescence emission spectra of other systems, XPS, CD. The Supporting Information is available free of charge on the ACS Publications website at DOI: 10.1021/acsami.5b00684.

■ AUTHOR INFORMATION

Corresponding Authors

*E-mail: zkzhang@nankai.edu.cn.

*E-mail: shilinqi@nankai.edu.cn. Fax: +86 22 23503510. Tel: +86 22 23506103.

Notes

The authors declare no competing financial interest.

■ ACKNOWLEDGMENTS

This work was supported by the National Natural Science Foundation of China (No. 21274067, 91127045, 51390483), the Fundamental Research Funds for the Central Universities, Natural Science Foundation of Tianjin, China (No. 12JCQNJC01800), and PCSIRT (IRT1257).

■ REFERENCES

(1) Wagner, V.; Dullaart, A.; Bock, A.-K.; Zweck, A. The Emerging Nanomedicine Landscape. *Nat. Biotechnol.* **2006**, *24* (10), 1211−1218.

(2) Farokhzad, O. C.; Langer, R. Nanomedicine: Developing Smarter Therapeutic and Diagnostic Modalities. *Adv. Drug Delivery Rev.* **2006**, *58* (14), 1456−1459.

(3) Mahmoudi, M.; Lynch, I.; Ejtehadi, M. R.; Monopoli, M. P.; Bombelli, F. B.; Laurent, S. Protein−Nanoparticle Interactions: Opportunities and Challenges. *Chem. Rev.* **2011**, *111* (9), 5610−5637.

(4) Lynch, I.; Dawson, K. A. Protein−Nanoparticle Interactions. *Nano Today* **2008**, *3* (1), 40−47.

(5) Owens, D. E., III; Peppas, N. A. Opsonization, Biodistribution, and Pharmacokinetics of Polymeric Nanoparticles. *Int. J. Pharm.* **2006**, *307* (1), 93−102.

(6) Gao, H.; Xiong, J.; Cheng, T.; Liu, J.; Chu, L.; Liu, J.; Ma, R.; Shi, L. In Vivo Biodistribution of Mixed Shell Micelles with Tunable Hydrophilic/Hydrophobic Surface. *Biomacromolecules* **2013**, *14* (2), 460−467.

DOI: 10.1021/acsami.5b00684
ACS Appl. Mater. Interfaces 2015, 7, 10238−10249

(7) Beierle, J. M.; Yoshimatsu, K.; Chou, B.; Mathews, M. A.; Lesel, B. K.; Shea, K. J. Polymer Nanoparticle Hydrogels with Autonomous Affinity Switching for the Protection of Proteins from Thermal Stress. *Angew. Chem., Int. Ed.* **2014**, *53* (35), 9275−9279.
(8) Liu, X.; Liu, Y.; Zhang, Z.; Huang, F.; Tao, Q.; Ma, R.; An, Y.; Shi, L. Temperature-Responsive Mixed-Shell Polymeric Micelles for the Refolding of Thermally Denatured Proteins. *Chem.—Eur. J.* **2013**, *19* (23), 7437−7442.
(9) Linse, S.; Cabaleiro-Lago, C.; Xue, W.; Lynch, I.; Lindman, S.; Thulin, E.; Radford, S. E.; Dawson, K. A. Nucleation of Protein Fibrillation by Nanoparticles. *Proc. Natl. Acad. Sci. U. S. A.* **2007**, *104* (21), 8691−8696.
(10) Hoshino, Y.; Urakami, T.; Kodama, T.; Koide, H.; Oku, N.; Okahata, Y.; Shea, K. J. Design of Synthetic Polymer Nanoparticles That Capture and Neutralize a Toxic Peptide. *Small* **2009**, *5* (13), 1562−1568.
(11) Ren, J.; Zhang, Y.; Zhang, J.; Gao, H.; Liu, G.; Ma, R.; An, Y.; Kong, D.; Shi, L. pH/Sugar Dual Responsive Core-Cross-Linked PIC Micelles for Enhanced Intracellular Protein Delivery. *Biomacromolecules* **2013**, *14* (10), 3434−3443.
(12) Fujioka-Kobayashi, M.; Ota, M. S.; Shimoda, A.; Nakahama, K.; Akiyoshi, K.; Miyamoto, Y.; Iseki, S. Cholesteryl Group- and Acryloyl Group-Bearing Pullulan Nanogel to Deliver BMP2 and FGF18 for Bone Tissue Engineering. *Biomaterials* **2012**, *33* (30), 7613−7620.
(13) Ge, Z.; Liu, S. Functional Block Copolymer Assemblies Responsive to Tumor and Intracellular Microenvironments for Site-Specific Drug Delivery and Enhanced Imaging Performance. *Chem. Soc. Rev.* **2013**, *42* (17), 7289−7325.
(14) Liu, D.; Yang, Q.; Jin, S.; Song, Y.; Gao, J.; Wang, Y.; Mi, H. Core−Shell Molecularly Imprinted Polymer Nanoparticles with Assistant Recognition Polymer Chains for Effective Recognition and Enrichment of Natural Low-Abundance Protein. *Acta Biomater.* **2014**, *10* (2), 769−775.
(15) You, C. C.; Miranda, O. R.; Gider, B.; Ghosh, P. S.; Kim, I. B.; Erdogan, B.; Krovi, S. A.; Bunz, U. H.; Rotello, V. M. Detection and Identification of Proteins Using Nanoparticle−Fluorescent Polymer "Chemical Nose" Sensors. *Nat. Nanotechnol.* **2007**, *2* (5), 318−323.
(16) Welsch, N.; Lu, Y.; Dzubiella, J.; Ballauff, M. Adsorption of Proteins to Functional Polymeric Nanoparticles. *Polymer* **2013**, *54* (12), 2835−2849.
(17) Yoshimatsu, K.; Lesel, B. K.; Yonamine, Y.; Beierle, J. M.; Hoshino, Y.; Shea, K. J. Temperature-Responsive "Catch and Release" of Proteins by Using Multifunctional Polymer-Based Nanoparticles. *Angew. Chem., Int. Ed.* **2012**, *51* (10), 2405−2408.
(18) Hoshino, Y.; Koide, H.; Urakami, T.; Kanazawa, H.; Kodama, T.; Oku, N.; Shea, K. J. Recognition, Neutralization, and Clearance of Target Peptides in the Bloodstream of Living Mice by Molecularly Imprinted Polymer Nanoparticles: A Plastic Antibody. *J. Am. Chem. Soc.* **2010**, *132* (19), 6644−6645.
(19) Sasaki, Y.; Akiyoshi, K. Nanogel Engineering for New Nanobiomaterials: From Chaperoning Engineering to Biomedical Applications. *Chem. Rec.* **2010**, *10* (6), 366−376.
(20) Welsch, N.; Becker, A. L.; Dzubiella, J.; Ballauff, M. Core−Shell Microgels as "Smart" Carriers for Enzymes. *Soft Matter* **2012**, *8* (5), 1428−1436.
(21) Huang, F.; Wang, J.; Qu, A.; Shen, L.; Liu, J.; Liu, J.; Zhang, Z.; An, Y.; Shi, L. Maintenance of Amyloid β Peptide Homeostasis by Artificial Chaperones Based on Mixed-Shell Polymeric Micelles. *Angew. Chem., Int. Ed.* **2014**, *53* (34), 8985−8990.
(22) Cedervall, T.; Lynch, I.; Lindman, S.; Berggård, T.; Thulin, E.; Nilsson, H.; Dawson, K. A.; Linse, S. Understanding the Nanoparticle−Protein Corona Using Methods to Quantify Exchange Rates and Affinities of Proteins for Nanoparticles. *Proc. Natl. Acad. Sci. U. S. A.* **2007**, *104* (7), 2050−2055.
(23) Klein, J. Probing the Interactions of Proteins and Nanoparticles. *Proc. Natl. Acad. Sci. U. S. A.* **2007**, *104* (7), 2029−2030.
(24) Zeng, Z.; Patel, J.; Lee, S. H.; McCallum, M.; Tyagi, A.; Yan, M.; Shea, K. J. Synthetic Polymer Nanoparticle−Polysaccharide Interactions: A Systematic Study. *J. Am. Chem. Soc.* **2012**, *134* (5), 2681−2690.
(25) Li, L.; Mu, Q.; Zhang, B.; Yan, B. Analytical Strategies for Detecting Nanoparticle−Protein Interactions. *Analyst* **2010**, *135* (7), 1519−1530.
(26) Röcker, C.; Pötzl, M.; Zhang, F.; Parak, W. J.; Nienhaus, G. U. A Quantitative Fluorescence Study of Protein Monolayer Formation on Colloidal Nanoparticles. *Nat. Nanotechnol.* **2009**, *4* (9), 577−580.
(27) Blagoi, G.; Rosenzweig, N.; Rosenzweig, Z. Design, Synthesis, and Application of Particle-Based Fluorescence Resonance Energy Transfer Sensors for Carbohydrates and Glycoproteins. *Anal. Chem.* **2005**, *77* (2), 393−399.
(28) Li, C.; Zhang, Y.; Hu, J.; Cheng, J.; Liu, S. Reversible Three-State Switching of Multicolor Fluorescence Emission by Multiple Stimuli Modulated FRET Processes within Thermoresponsive Polymeric Micelles. *Angew. Chem.* **2010**, *122* (30), 5246−5250.
(29) Okada, K.; Maeda, Y. Thermochromic Microgels and Core-Shell Microgels Based on Fluorescence Resonance Energy Transfer. *J. Appl. Polym. Sci.* **2013**, *130* (1), 201−205.
(30) Ma, C.; Zeng, F.; Huang, L.; Wu, S. FRET-Based Ratiometric Detection System for Mercury Ions in Water with Polymeric Particles as Scaffolds. *J. Phys. Chem. B* **2011**, *115* (5), 874−882.
(31) Quadir, M. A.; Morton, S. W.; Deng, Z. J.; Shopsowitz, K. E.; Murphy, R. P.; Epps, T. H.; Hammond, P. T. PEG−Polypeptide Block Copolymers as pH-Responsive Endosome-Solubilizing Drug Nanocarriers. *Mol. Pharmaceutics* **2014**, *11* (7), 2420−2430.
(32) Lu, J.; Owen, S. C.; Shoichet, M. S. Stability of Self-Assembled Polymeric Micelles in Serum. *Macromolecules* **2011**, *44* (15), 6002−6008.
(33) Selvin, P. R. The Renaissance of Fluorescence Resonance Energy Transfer. *Nat. Struct. Biol.* **2000**, *7* (9), 730−734.
(34) Muthuraj, B.; Deshmukh, R.; Trivedi, V.; Iyer, P. K. Highly Selective Probe Detects Cu^{2+} and Endogenous NO Gas in Living Cell. *ACS Appl. Mater. Interfaces* **2014**, *6* (9), 6562−6569.
(35) Morton, S. W.; Zhao, X.; Quadir, M. A.; Hammond, P. T. FRET-Enabled Biological Characterization of Polymeric Micelles. *Biomaterials* **2014**, *35* (11), 3489−3496.
(36) Li, G.; Shi, L.; Ma, R.; An, Y.; Huang, N. Formation of Complex Micelles with Double-Responsive Channels from Self-Assembly of Two Diblock Copolymers. *Angew. Chem.* **2006**, *118* (30), 5081−5084.
(37) Ma, R.; Wang, B.; Xu, Y.; An, Y.; Zhang, W.; Li, G.; Shi, L. Surface Phase Separation and Morphology of Stimuli Responsive Complex Micelles. *Macromol. Rapid Commun.* **2007**, *28* (9), 1062−1069.
(38) Liu, X.; Ma, R.; Shen, J.; Xu, Y.; An, Y.; Shi, L. Controlled Release of Ionic Drugs from Complex Micelles with Charged Channels. *Biomacromolecules* **2012**, *13* (5), 1307−1314.
(39) Chen, X.; Wang, X.; Wang, S.; Shi, W.; Wang, K.; Ma, H. A Highly Selective and Sensitive Fluorescence Probe for the Hypochlorite Anion. *Chem.—Eur. J.* **2008**, *14* (15), 4719−4724.
(40) Hiramatsu, M.; Okabe, N.; Tomita, K. i. Preparation and Properties of Lysozyme Modified by Fluorescein-Isothiocyanate. *J. Biochem.* **1973**, *73* (5), 971−978.
(41) Robeson, J. L.; Tilton, R. D. Spontaneous Reconfiguration of Adsorbed Lysozyme Layers Observed by Total Internal Reflection Fluorescence with a pH-Sensitive Fluorophore. *Langmuir* **1996**, *12* (25), 6104−6113.
(42) Chang, J. Y.; Li, L. The Unfolding Mechanism and the Disulfide Structures of Denatured Lysozyme. *FEBS Lett.* **2002**, *511* (1), 73−78.
(43) Ibrahim, H. R.; Higashiguchi, S.; Juneja, L. R.; Kim, M.; Yamamoto, T. A Structural Phase of Heat-Denatured Lysozyme with Novel Antimicrobial Action. *J. Agric. Food Chem.* **1996**, *44* (6), 1416−1423.
(44) Rozema, D.; Gellman, S. H. Artificial Chaperone-Assisted Refolding of Denatured-Reduced Lysozyme: Modulation of the Competition between Renaturation and Aggregation. *Biochemistry* **1996**, *35* (49), 15760−15771.
(45) Yu, B.; Chan, J. W.; Hoyle, C. E.; Lowe, A. B. Sequential Thiol-Ene/Thiol-Ene and Thiol-Ene/Thiol-Yne Reactions as a Route to

DOI: 10.1021/acsami.5b00684
ACS Appl. Mater. Interfaces 2015, 7, 10238−10249

Well-Defined Mono and Bis End-Functionalized Poly(*N*-Isopropylacrylamide). *J. Polym. Sci., Part A: Polym. Chem.* **2009**, *47* (14), 3544−3557.
(46) Zhang, Z.; Ma, R.; Shi, L. Cooperative Macromolecular Self-Assembly toward Polymeric Assemblies with Multiple and Bioactive Functions. *Acc. Chem. Res.* **2014**, *47* (4), 1426−1437.
(47) Mine, Y.; Noutomi, T.; Haga, N. Thermally Induced Changes in Egg White Proteins. *J. Agric. Food Chem.* **1990**, *38* (12), 2122−2125.
(48) Makki, F.; Durance, T. D. Thermal Inactivation of Lysozyme as Influenced by pH, Sucrose and Sodium Chloride and Inactivation and Preservative Effect in Beer. *Food Res. Int.* **1996**, *29* (7), 635−645.
(49) Hu, Z.; Hu, J.; Cui, Y.; Wang, G.; Zhang, X.; Uvdal, K.; Gao, H. W. A Facile "Click" Reaction to Fabricate a FRET-Based Ratiometric Fluorescent Cu^{2+} Probe. *J. Mater. Chem. B* **2014**, *2* (28), 4467−4472.
(50) Piston, D. W.; Kremers, G. J. Fluorescent Protein FRET: The Good, the Bad and the Ugly. *Trends Biochem. Sci.* **2007**, *32* (9), 407−414.
(51) Socher, E.; Imperiali, B. FRET-Capture: A Sensitive Method for the Detection of Dynamic Protein Interactions. *ChemBioChem* **2013**, *14* (1), 53−57.
(52) Kong, H. J.; Kim, C. J.; Huebsch, N.; Weitz, D.; Mooney, D. J. Noninvasive Probing of the Spatial Organization of Polymer Chains in Hydrogels Using Fluorescence Resonance Energy Transfer (FRET). *J. Am. Chem. Soc.* **2007**, *129* (15), 4518−4519.
(53) Gref, R.; Lück, M.; Quellec, P.; Marchand, M.; Dellacherie, E.; Harnisch, S.; Blunk, T.; Müller, R. "Stealth" Corona−Core Nanoparticles Surface Modified by Polyethylene Glycol (PEG): Influences of the Corona (PEG Chain Length and Surface Density) and of the Core Composition on Phagocytic Uptake and Plasma Protein Adsorption. *Colloids Surf., B* **2000**, *18* (3), 301−313.

DOI: 10.1021/acsami.5b00684
ACS Appl. Mater. Interfaces 2015, 7, 10238−10249